

Retrieval of optical constants and thickness of thin films from transmission spectra

I. Chambouleyron, J. M. Martínez, A. C. Moretti, and M. Mulato

We discuss a new method to estimate the absorption coefficient, the index of refraction, and the thickness of thin films using optical transmission data only. To solve the problem we used a pointwise constrained optimization approach, defining a nonlinear programming problem, the unknowns of which are the coefficients to be estimated, with linear constraints that represent prior knowledge about the physical solution. The method applies to all kinds of transmission spectra and does not rely on the existence of fringe patterns or transparency. Results on amorphous semiconductor thin films and gedanken films are reported. They show that the new method is highly reliable. © 1997 Optical Society of America

1. Introduction

Since the advent of microelectronics and advanced optical devices, the use of thin dielectric and semiconductor films has spread considerably. Thin-film electronics, which includes thin-film transistors and amorphous semiconductor solar cells, and interferometric tailor-made optical filters are among the most common applications. In many cases the thickness d and the optical properties [$\tilde{n}(\lambda) = n(\lambda) + ik(\lambda)$; the symbols have their usual meaning] of homogeneous films must be known with some degree of accuracy. Measurements of the complex amplitudes of the light transmitted by films deposited upon transparent substrates of known refractive index and of the light reflected at normal or oblique incidence at the film and substrate sides or different combinations of these conditions enable the explicit evaluation of the thickness and the optical constants in a broad spectral range.^{1,2} For most applications, however, the interesting photon energy range covers the neighborhood of the fundamental absorption edge, or optical gap, in which the material goes from complete opacity to some degree of transparency. Because optical transmittance provides accurate and quick information on

this spectral range, efforts have been made to develop methods that allow the retrieval of the thickness and the optical constants of thin films from transmission data only.³⁻⁵

Figure 1 shows three typical transmission spectra of thin isotropic and homogeneous films, bounded by plane-parallel surfaces and deposited onto transparent finite substrates. They correspond to (a) a dielectric film, thick enough to display interference fringes that come from multiple coherent reflections at the interfaces and that possesses a highly transparent region below the fundamental absorption edge energy; (b) a thick film, as above, but strongly absorbing over all the measured spectral range; and (c) a very thin film that does not show any fringe pattern.

The interference fringes of films with a transparent spectral region, such as those shown by film (a) (Fig. 1), can be used to estimate the film thickness and the real part of the index of refraction in the transparent region.¹⁻⁵ The calculation of the optical constants in the absorbing region, however, cannot be estimated in a simple way. Usually a functional dependence for $n(\lambda)$ is assumed, in most cases a function of the type $n = A\lambda^{-2} + B\lambda + C$ (where A , B , and C are constants), for extrapolating the index values estimated in the transparent region of the spectrum to higher photon energies. If d and $n(\lambda)$ are known, the absorption coefficient can be estimated from the general expression of the transmission. In general, these approximations are of limited accuracy and result in a poor estimate of the absorption coefficient. Films that do not possess a transparent spectral region or that are too thin to display optical fringes in the measured range cannot be solved by these ap-

I. Chambouleyron and M. Mulato are with the Instituto de Física Gleb Wataghin, Universidade Estadual de Campinas-UNICAMP, 13083-970 Campinas, SP, Brazil. J. M. Martínez and A. C. Moretti are with the Instituto de Matemática, Universidade Estadual de Campinas-UNICAMP, 13083-970 Campinas, SP, Brazil.

Received 24 March 1997; revised manuscript received 16 June 1997.

0003-6935/97/318238-10\$10.00/0

© 1997 Optical Society of America

proximate methods, which use transmission data only [films (b) and (c) of Fig. 1, for example].

We consider the problem from a different point of view. Instead of assuming that $n(\lambda)$ and $\alpha(\lambda)$ at different wavelengths are linked by a functional relation, we establish explicitly the physical constraints that n and α must satisfy in the spectral region where optical transmission data are available. The method consists of defining a nonlinear programming problem, the unknowns of which are the coefficients to be estimated, with linear constraints that represent a prior knowledge about the physical solution. For solving the problem a pointwise constrained optimization approach is used. The reliability of the method is tested with numerical experiments with computer-generated transmission data of films of known optical constants and thickness. The results of the retrieval process of the optical constants and the thickness of these computer-made films, or Gedanken experiments, show that the new method is highly reliable even in the case of absorbing films or of films that show no fringe pattern in their optical transmittance. The method is used afterward to calculate the optical constants and the thickness of amorphous semiconductor thin films deposited upon glass and crystalline silicon substrates with the use of measured transmission data only. The calculated values are compared with the optical parameters determined from independent methods. A good agreement is found in the case of homogeneous films.

2. Description of Method

The optical transmission of a thin absorbing film deposited on a transparent substrate is given by¹

$$T = \frac{Ax}{B - Cx + Dx^2}, \quad (1)$$

where

$$A = 16s(n^2 + k^2), \quad (2)$$

$$B = [(n + 1)^2 + k^2][(n + 1)(n + s^2) + k^2], \quad (3)$$

$$C = [(n^2 - 1 + k^2)(n^2 - s^2 + k^2) - 2k^2(s^2 + 1)]2 \times \cos \varphi - k[2(n^2 - s^2 + k^2) + (s^2 + 1) \times (n^2 - 1 + k^2)]2 \sin \varphi, \quad (4)$$

$$D = [(n - 1)^2 + k^2][(n - 1)(n - s^2) + k^2], \quad (5)$$

$$\varphi = 4\pi nd/\lambda, \quad x = \exp(-\alpha d), \quad \alpha = 4\pi k/\lambda. \quad (6)$$

In Eqs. (2)–(6) the following notation is used:

- (1) λ is the wavelength;
- (2) $s(\lambda)$, the refractive index of the thick transparent substrate, is a slowly varying function of λ and can be calculated from the transmission of the bare substrate T_s :

$$T_s = \frac{2s}{s^2 + 1}, \quad \text{or} \quad s = \frac{1}{T_s} + \left(\frac{1}{T_s^2} - 1 \right)^{1/2}; \quad (7)$$

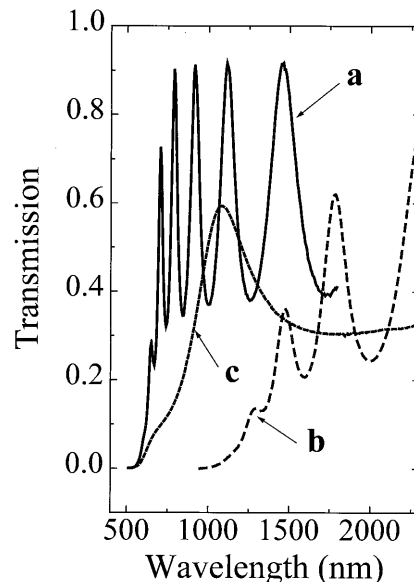


Fig. 1. Typical transmission spectra in the visible and near-infrared wavelength range of thin dielectric films deposited onto a transparent substrate; film (a) is transparent at $\lambda > 1000$ nm and thick enough to display a fringe pattern, film (b) absorbs over the whole measured range, and film (c) is thin and does not show any interference pattern.

(3) $n = n(\lambda)$ is the real part of the refractive index of the film;

(4) $\alpha = \alpha(\lambda) = 4\pi k(\lambda)/\lambda$ is the absorption coefficient of the film, $k(\lambda)$ being the extinction coefficient, and;

(5) d is the thickness of the film that has to be uniform and homogeneous, otherwise interference effects are destroyed or severely affected.

A set of experimental data (λ_i, T_i) , $i = 1, 2, \dots, N$, ($\lambda_i < \lambda_{i+1}$ for all $i = 1, \dots, N$) is available from the measured transmittance. From the data d , $n(\lambda)$ and $\alpha(\lambda)$ are to be determined. At first sight, the problem is highly underdetermined. Even with the assumption that d is known, for all $i = 1, \dots, N$, the following equation must hold:

$$T[\lambda_i, s(\lambda_i), d, n(\lambda_i), \alpha(\lambda_i)] = T_i. \quad (8)$$

Equation (8) has two unknowns, $n(\lambda_i)$ and $\alpha(\lambda_i)$, and its set of solutions is in general a curve in the $[n(\lambda_i), \alpha(\lambda_i)]$ space. Therefore the set of functions (n, α) that satisfy Eq. (8) for a given d is infinite and, roughly speaking, is represented by a nonlinear manifold of dimension N in \mathbf{R}^{2N} .

As already mentioned, the usual approach for the estimation of n and α consists of assuming functional forms, with few parameters, for $n(\lambda)$ and $\alpha(\lambda)$ and estimating the unknown parameters with nonlinear least-squares methods or *ad hoc* procedures.⁵ In general these procedures give unacceptable errors⁶ if the true functional form of $n(\lambda)$ and $\alpha(\lambda)$ is not known, as usual in practical cases.

In the present analysis, a different point of view is adopted. The type of constraints that relate n and α at different wavelengths derive from a prior knowl-

edge about the physical solution. To illustrate the approach, let us consider, for example, the behavior of the optical constants of an amorphous (a-) semiconductor thin film. In the neighborhood of the fundamental absorption edge of a-semiconductors it is known that [from now on $n_i = n(\lambda_i)$, $\alpha_i = \alpha(\lambda_i)$, to simplify the notation]:

$$(a) \alpha_i \geq 0 \text{ and } n_i \geq 1 \text{ for all } i = 1, \dots, N. \quad (9)$$

(b) The functions $\alpha(\lambda)$ and $n(\lambda)$ are decreasing; so, for all $i = 1, \dots, N - 1$,

$$\alpha_{i+1} \leq \alpha_i \text{ and } n_{i+1} \leq n_i. \quad (10)$$

(c) In the $T \geq 0$ region, $n(\lambda)$ is a convex function,⁷ i.e., $n''(\lambda) \geq 0$, or

$$n_i \leq n_{i-1} + \frac{n_{i+1} - n_{i-1}}{\lambda_{i+1} - \lambda_{i-1}} (\lambda_i - \lambda_{i-1}). \quad (11)$$

(d) In a $\log(\alpha)$ versus $\hbar\omega$ (photon energy) plot, the absorption coefficient α of an a-semiconductor has an elongated S-like shape.⁷ Thus for a spectral region that corresponds to the exponential absorption edge and smaller photon energies, $\alpha(\lambda)$ is also a convex function $\alpha''(\lambda) \geq 0$, or

$$\alpha_i \leq \alpha_{i-1} + \frac{\alpha_{i+1} - \alpha_{i-1}}{\lambda_{i+1} - \lambda_{i-1}} (\lambda_i - \lambda_{i-1}). \quad (12)$$

The constraints (a), (b), (c), and (d) above relate unknowns of Eq. (8) for different indices i . Therefore Eq. (8) can no longer be considered independent and the degrees of freedom are restricted. From the above considerations, we model the problem of determining d , n , and α in a selected spectral region with the following optimization procedure:

$$\text{Minimize } \sum_{i=1}^N [T_i - T(\lambda_i, s, d, n_i, \alpha_i)]^2, \quad (13)$$

subject to constraints (a), (b), (c), and (d). For obvious reasons, this is called a pointwise constrained optimization approach for the resolution of the estimation problem.

For a given value of the thickness d , the constraints (a), (b), (c), and (d) define a polyhedron \mathbf{P} with nonempty interior in \mathbf{R}^{2N} . (The discretization of any pair of nonnegative, strictly convex and decreasing functions n and α is an interior point of \mathbf{P}). Therefore the intersection of \mathbf{P} with the set of points that satisfies Eq. (8) is nonempty and defines a set of \mathbf{R}^{2N} that, in general, contains more than one point. In principle, a global solution of expressions (9)–(13) could not be a unique solution of the estimation problem (which clearly exists in real world situations because of physical reasons and exists in numerical experiments by construction). However, if the intersection of \mathbf{P} with the set defined by Eq. (8) is small, we can expect that any (approximate) solution of expressions (9)–(13) is the closest to the true solution of the

estimation problem. Theoretical verification of this fact is difficult or even impossible except for small values of N , but an experimental study can be designed to establish the reliability of the pointwise constrained optimization approach.

The nonlinear programming⁸ of expressions (9)–(13) with linear constraints, where the number of variables is $2N$ (for a given d) and the number of constraints is $2(N - 1) + 2(N - 2) = 4N - 6$ [excluding expression (9)], is solved with the code MINOS, a well-known piece of software developed at Stanford University for solving large-scale linearly constrained nonlinear programming problems.^{9–11} The first version of MINOS appeared in 1977 and successive updates have been produced since.

In Section 3 we apply the above procedure to the optical transmission data of computer-generated films of known optical properties and thickness deposited onto a transparent substrate of known index of refraction. We evaluate the accuracy of the retrieval process by comparing the retrieved values with the known solution. All our computations were done in a Sparc Station 2 with a 32-bit processor, 28.5 MIPS, 4.2 MFLOPS, and 32 Mbytes of RAM.

3. Numerical Experiments with Computer-Made Films

For λ_i (nm) = 500 + $(i - 1)$, $i = 1, \dots, 500$, we generate transmission data with Eqs. (1)–(6) for two different films of thickness, $d_1 = 100$ nm and $d_2 = 600$ nm, respectively. These gedanken experiments are intended to simulate representative films for electronic applications. The transmission data, generated in the 500–1000-nm wavelength range, are rounded off to three digits to mimic the precision of the information normally available with experimental data. The simulation includes a glass substrate, assumed to be transparent in the spectral range under consideration. The example considers the following functional dependence for the optical constants of films and substrate:

$$\begin{aligned} n_i &= [1 + (0.09195 - 12600/\lambda_i^2)^{-1}]^{1/2}, \\ \alpha_i (\text{nm}^{-1}) &= 10^{-3} \times \exp[(24780/\lambda_i) - 34], \\ s_i &= [1 + (0.7568 - 7930/\lambda_i^2)^{-1}]^{1/2}, \end{aligned}$$

where λ_i is given in nanometers and α in inverse nanometers. The absorption coefficient of the film has an exponential dependence on photon energy. The idea behind this particular choice of a rather steep α is to investigate the power of the method for the retrieval of small and large α 's. The transmittance of film No. 1 and film No. 2 is shown in Fig. 2. As expected, film No. 1 does not show any fringe pattern in this spectral range. Owing to the photon energy dependence of the adopted α and the film thickness, no transmission $T > 10^{-3}$ is measured for $\lambda < 650$ nm. Because the transmission data are generated every nanometer wavelength, we are left with 350 equations for the optimization process. Note that with only the transmission data of the

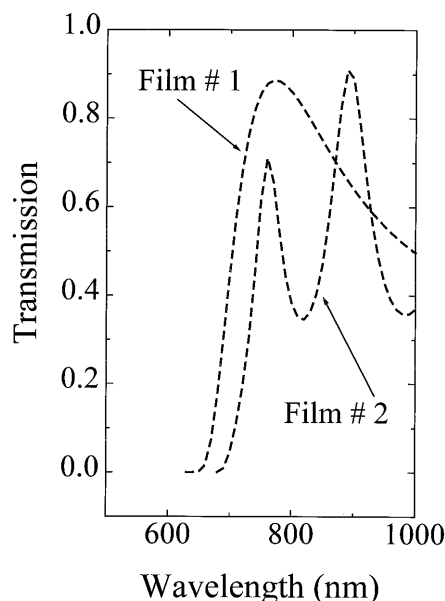


Fig. 2. Transmittance against wavelength of computer-made film No. 1 ($d = 100$ nm) and film No. 2 ($d = 600$ nm). The transmission data, rounded off to three digits, are used to retrieve their thickness and optical constants.

$650 < \lambda < 1000$ -nm range none of the films under consideration can be solved by approximate methods.

We solve expressions (9)–(13) with the generated transmission data for different values of the film thickness d . Table 1 provides the optimal values obtained for the objective function by MINOS for all the thicknesses tested. The least value of the quadratic error corresponds to the true film thickness. In all the tests we used the following initial guesses for n and α : $n_i = -6 \times 10^{-4} \lambda_i + 4.3$ and $\alpha_i = -0.0242 \lambda_i + 24.2$, which are far from the true values (see Fig. 3).

Figures 3a and 3b show the optical constants of the

Table 1. Results of Minimization Process^a on Computer-Made Dielectric Films Deposited onto Glass

Film 1		Film 2	
Thickness (nm)	Minimization	Thickness (nm)	Minimization
50	2.403	540	0.1598
60	6.654	550	2.9014
70	2.27	560	0.05537
80	0.215	570	0.02765
90	0.02564	580	0.01129
100 ^b	1.587×10^{-5}	590	0.0025
110	0.01773	600 ^b	1.823×10^{-5}
120	0.1722	610	0.9925
130	0.4584	620	0.874
140	2.2687	630	1.9843
150	2.2358	640	0.038
		650	3.908
		660	0.10004

^a $\sum_{i=1}^N [T_i - T(\lambda_i, s, d, n_i, \alpha_i)]^2$

^bNote the absolute minimum at the true film thickness values, i.e., $d = 100$ nm (film 1) and $d = 600$ nm (film 2).

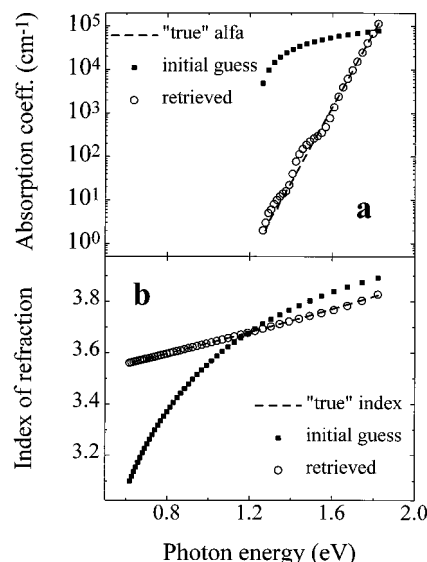


Fig. 3. Retrieved values of the (a) absorption coefficient and the (b) index of refraction for the gedanken film No. 2 in Fig. 2 against photon energy; the retrieved values are compared with the true values used to generate the transmission data. Note the overall excellent agreement of both. The initial guesses for α and n are also shown.

gedanken films as a function of photon energy as given by the minimization process at the optimum thickness. They are compared with the true values used to generate the transmission data and with the initial guesses for n and α used in the minimization process. The accuracy of the retrieval is outstanding. For the sake of clarity, only the data corresponding to film No. 2 are shown in Fig. 3; the values found for film No. 1 are essentially the same. Let us first discuss the retrieval of the absorption coefficient α .

Figure 3a indicates that within a factor of less than 2 the absorption coefficient has been retrieved in a range of 5 orders of magnitude, from approximately 1 cm^{-1} to more than 10^5 cm^{-1} . Note that this is for a 600-nm-thick film. For the index of refraction, Fig. 3b also shows an excellent retrieval for all the $0.001 \leq T \leq 0.999$ range. Let us stress that the almost perfect agreement between true optical constants and the retrieved values has been tested in a variety of situations that includes films of different thicknesses that are deposited onto different substrates. The retrieval of α for film No. 1 gives results similar to those of Fig. 3a, the only difference being that the curve of the retrieved α is shifted along the true value curve a little upward, i.e., the retrieval fails at $\alpha \approx 10 \text{ cm}^{-1}$ instead of $\alpha \approx 1 \text{ cm}^{-1}$ as in Fig. 3a. On the other hand, α is retrieved up to values higher than those shown in Fig. 3a. This is an indication that αd governs the retrieval of the absorption coefficient in the $10^{-3} \leq T \leq 0.999$ spectral range, as expected.

Some important remarks are in order at this point:

- The numerical examples have been computed with transmission data rounded off to three digits,

i.e., $10^{-3} \leq T \leq 0.999$. The number of available significant digits limits the precision of the retrieval process.

- The relative error associated with the rounding off of transmission values increases considerably as $T \rightarrow 0$. This unavoidable fact perturbs the retrieval of the true thickness if all $T > 0$ data points are considered in the minimization process. To circumvent the problem, the minimization process [expressions (9)–(13)] that leads to the best film thickness is made with only transmission data larger than a selected value, say $T > 20\%$. We call T_{cut} the minimum transmission to be used in the minimization process. Simulations were made with different T_{cut} values and $T_{\text{cut}} = 10\%$ was found satisfactory for gedanken films. The results of calculations, shown in Table 1, correspond to the minimization process performed with only $T > 10\%$ data. When the best thickness is found, the optical constants of gedanken films in the remaining absorbing spectral region are calculated with Eqs. (1)–(6) and constraints (9)–(12), keeping the best thickness in the process. As we discuss in Subsection 4.A, T_{cut} is also a useful tool to help define spectral transmission regions where the strongest constraints on n and α may be imposed, easing the minimization process.

- We are dealing with an ideal situation in the sense that computer-generated transmission data contain only rounding-off errors but no systematic or random errors that are always present in measured transmission. For instance, the numerical examples consider transmission data that correspond to pure wavelengths, i.e., $\Delta\lambda = 0$ (no bandwidth effects). A finite $\Delta\lambda$, unavoidable in experimental cases, tends to shrink interference fringes. Moreover, because the coherence length² ($\Lambda = \lambda^2/\Delta\lambda$) is infinite in our computer experiments, interference effects should appear on any substrate of finite thickness. These effects were not considered in the present numerical examples but should influence the outcome of the retrieval process from experimental transmission data. It is fortunate that many of them may be taken care of conveniently in the equations of the minimization process.⁵

4. Amorphous Semiconductor Thin Films

We discuss now the pointwise constrained optimization approach applied to the measured optical transmission of amorphous silicon and germanium thin films. As compared with gedanken films, the analysis of real film data possesses both advantages and drawbacks. The main advantage is that the deposited material is known, and from its known properties it is possible to impose constraints on α and n that are valid in selected spectral regions. In this way the overall problem may be solved by parts, as is explained in what follows. Moreover the knowledge of the film's material also allows a relatively good initial guess for $\alpha(\lambda)$ and $n(\lambda)$, which may help to speed the minimization process. Finally, from the deposition rate, Talystep measurements, and/or the presence or absence of a fringe pattern, a good initial

guess for the thickness of the film can be made. Thus the search for the best thickness d (minimization) can be computed in a reduced thickness interval.

The drawbacks stem from the unavoidable presence of errors in the experimental data. Besides the errors associated to the possible nonparallelism of the film faces, inhomogeneity of the material, and surface roughness, all measurements are made in spectrophotometers with finite slits. At any given wavelength an average intensity, corresponding to a band $\pm(\Delta\lambda)$ around λ , is measured. The consequence of a finite bandwidth $\Delta\lambda$ is the shrinkage of the fringe pattern; the effect is larger the thicker the film. The quality of experimental data worsens with increasing $\Delta\lambda$ and with decreasing wavelength. Finally, there may also be systematic errors resulting from mechanical or detector calibration deficiencies.

The characteristic feature of a-semiconductors is topological disorder (lack of long range order). Disorder induces the appearance of localized electron states in the neighborhood of the valence and conduction band extrema, which fall off exponentially with energy.⁷ Another consequence of disorder is the relaxation of the crystal momentum (\mathbf{k}) conservation rule in optical transitions.^{7,12} Coordination defects, or dangling bonds, create deep electron states that dominate the subgap absorption. Important variations that depend on preparation method and deposition conditions occur on the abruptness of the absorption edge and on the subgap absorption in a-semiconductors.¹³

During recent decades, tetrahedrally coordinated amorphous semiconductors have been the subject of intense research.¹⁴ Hydrogenated alloys of silicon (a-Si:H) and/or germanium (a-Si_xGe_{1-x}:H) are electronic materials in the sense that their electrical properties may be controlled by chemical doping. Their practical interest stems from the fact that they are useful materials for large-area electronic applications and as active layers of thin-film solar cells. In solar applications the optical constants and thicknesses of the films determine the amount of light that contributes to the photovoltaic conversion process. As already mentioned, the $\log[\alpha(\hbar\omega)]$ against the $\hbar\omega$ plot of the absorption edge of tetrahedrally coordinated amorphous semiconductors has an elongated S-like shape. The subgap absorption plateau, $0.1 < \alpha < 10 \text{ cm}^{-1}$, depends on the material's quality and gives an indication of the density of deep defects. At increasing photon energies, corresponding typically to $10\text{--}100 \text{ cm}^{-1} \leq \alpha \leq 10^3\text{--}10^4 \text{ cm}^{-1}$, the absorption coefficient depends exponentially on photon energy. At still larger photon energies α tends to saturate and it becomes a slowly increasing function of energy.^{12,14}

The study of the exponential absorption edge of amorphous semiconductors is of particular relevance for photoelectronic applications.^{14,15} Up to now, spectroscopic techniques have been of little use in determining the absorption coefficient of thin films in the weakly absorbing spectral region ($\alpha < 10^3 \text{ cm}^{-1}$). Methods like photothermal deflection spectroscopy

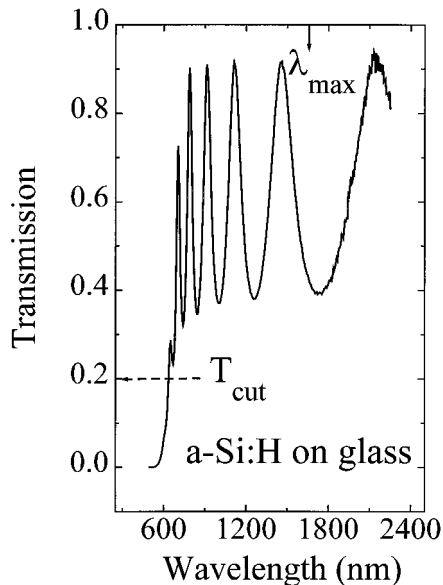


Fig. 4. Transmittance versus wavelength of an a-Si:H film deposited onto a Corning 7059 glass substrate. The noisy data at $\lambda > 1745$ nm have not been considered in the optimization process. See the text, Subsection 4.A, for the use of T_{cut} in the calculation of the film thickness and the optical constants.

(PDS),¹⁶ that are based on photothermal effects have been developed; a signal is measured related to the heat generated in the sample resulting from photon absorption. It is a sensitive though complex technique, requiring a calibration constant to give absolute absorption figures.

A. Hydrogenated Amorphous Silicon Films

We applied the pointwise constrained optimization method of the present contribution to the transmission data of a-semiconductor thin films. Figure 4 shows the transmittance of an a-Si:H film deposited by the glow discharge of SiH_4 onto a Corning 7059 glass substrate. The transmission data points (one every 3 nm) in the 500–2250-nm wavelength range were measured in a Hitachi Model U3410 spectrophotometer with $\Delta\lambda = 4$ nm and a scan speed of 30 nm/min. From the deposition rate and the deposition time the thickness of the film was estimated to be ≈ 600 nm. The retrieval of the optical constants and the thickness process was performed in two steps.

First, optimization (13) was performed with the 389 data points of the 578–1745-nm wavelength interval. This particular range was chosen because, as Fig. 4 shows, the data become noisy for $\lambda > \lambda_{\text{max}} = 1745$ nm; and $\lambda_{\text{min}} = 578$ nm corresponds to $T_{\text{cut}} = 0.2$. The known optical constants of a-Si:H and the estimated film thickness suggest that for transmission values $T > T_{\text{cut}}$ the absorption coefficient may be considered a convex function of λ . This being the case, it is possible to apply in the 578–1745-nm wavelength interval the constraints of convexity to both n

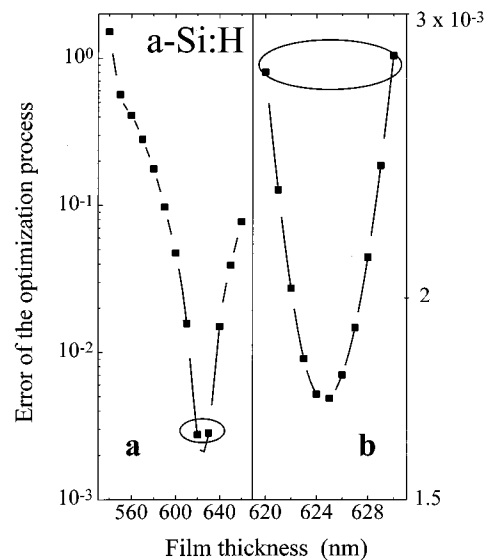


Fig. 5. Minimization process [expression (13)] that leads to the best film thickness: a, calculation with a coarse scan step (10 nm) in the 540–660-nm thickness range; b, deep minimum found at 625 nm with a fine (1-nm) scan step calculation in the 620–630-nm thickness range. It corresponds to the true film thickness. Note that Fig. 5b is an enlargement of the minimum seen in Fig. 5a.

and α . A reliable thickness d is retrieved in this way. The results appear in Fig. 5, where

$$\sum_{i=1}^N [T_i - T(\lambda_i, s, d, n_i, \alpha_i)]^2$$

versus thickness d has been plotted. Figure 5a shows the results of a coarse 10-nm step scan. Figure 5b is an enlargement of the minimum error region of Fig. 5a obtained with a smaller (1 nm) scan step. The absolute minimum, at 625 nm, of Fig. 5b indicates the best retrieved thickness. Its value is close to the value estimated from deposition rate and deposition time.

Second, when $d = 625$ nm is found and the optical constants in the 578–1745-nm wavelength interval are retrieved, we optimize the values of α and n for $\lambda < 578$ nm, keeping $d = 625$ nm in the calculations and relaxing the constraint of convexity on α . Figures 6a and 6b show the retrieved $\alpha(\lambda)$ and $n(\lambda)$ curves as a function of photon energy in the whole measured spectral range. Contrary to the case of gedanken films, we do not now have true $\alpha(\lambda)$ and $n(\lambda)$ values to compare with. Instead we compare the retrieved optical constants with the values obtained from independent measurements. Fig. 6a shows normalized PDS data, measured on the same a-Si:H/glass film. The good fitting between the retrieved $\alpha(\lambda)$ and the PDS data in the exponential absorption edge region is an independent test of the reliability of the calculation approach under discussion. Note that the calculation has been able to retrieve the true absorption edge down to absorption values of $\approx 100 \text{ cm}^{-1}$, a remarkably low figure if we consider that $\alpha(\lambda)$ has been obtained from the optical

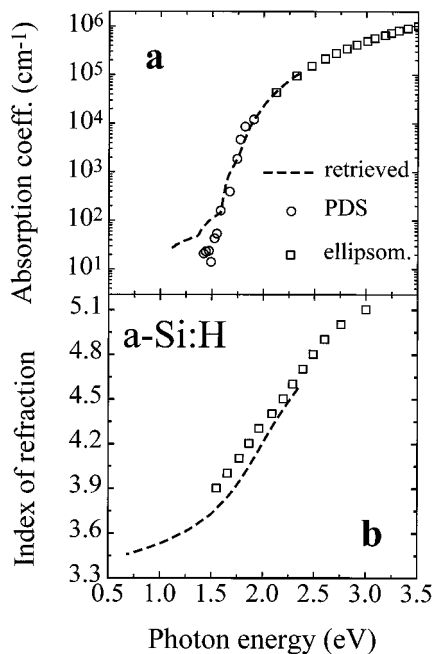


Fig. 6. a, Absorption coefficient; and b, index of refraction of a 625-nm-thick a-Si:H film versus photon energy retrieved from the transmission data of Fig. 4. The retrieved absorption is compared with PDS data normalized at $\alpha = 10^4 \text{ cm}^{-1}$ and with the absorption deduced from ellipsometry on an identical film deposited onto a c-Si substrate. The overall agreement for both optical constants is very good. Note that the pointwise constrained optimization approach retrieves an exponential absorption tail down to $\alpha \cong 100 \text{ cm}^{-1}$.

transmission data of a 625-nm-thick film. We believe that the differences between the calculated absorption and the normalized PDS values apparent for $\alpha < 100 \text{ cm}^{-1}$ (see Fig. 6a) are partly the consequence of the neglect of bandwidth errors in transmission data. Figure 6a also shows the absorption coefficient of an a-Si:H film deposited onto c-Si in the same deposition run, as determined from ellipsometry. The agreement between both sets of experimental data is excellent.

The retrieved values of $n(\lambda)$ are consistent with published values of n for a-Si:H films.¹⁵ The index values are plotted in Fig. 6b and compared with the data furnished by ellipsometry on the above-mentioned a-Si:H sample deposited onto c-Si in the same deposition run. Again the comparison shows the goodness of the present retrieval method in the photon energy region that corresponds to optical transmission. The dispersion of the refractive index of amorphous materials can be fitted by the Wemple-DiDomenico relation^{17,18}: $n^2 = 1 + \{E_d E_0 / [E_0^2 - (\hbar\omega)^2]\}$, where E_d and E_0 are single oscillator fitting constants that measure the oscillator energy and strength, respectively. If we plot the retrieved n values as $(n^2 - 1)^{-1}$ against $(\hbar\omega)^2$, a straight line results. From its slope and its intercept with the vertical axis, the values of E_d and E_0 of a-Si:H film can be determined, the oscillator energy E_0 being an average energy gap. In the present case $E_0 = 3.2 \text{ eV}$ is found, which roughly corresponds to the peak energy of the

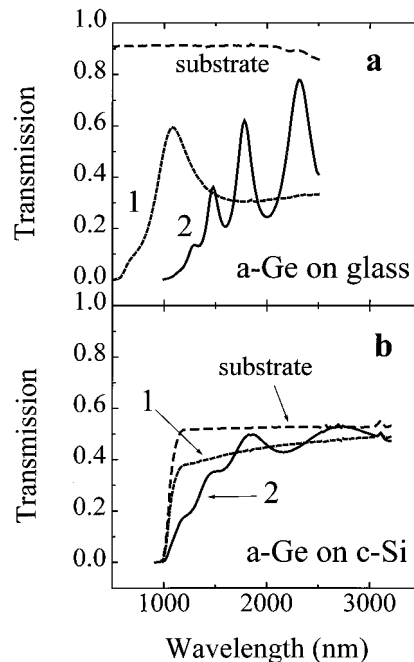


Fig. 7. a, Optical transmission of two a-Ge films deposited onto Corning 7059 glass; the thicknesses of film No. 1 and film No. 2 are estimated from the deposition rate to be approximately 100 and 600 nm thick, respectively; b, same a-Ge films deposited in the same run onto crystalline silicon (c-Si) substrates; the transmission of glass and c-Si is also shown.

imaginary part of the dielectric constant of amorphous silicon.¹⁹

B. H-Free Amorphous Germanium Films

Because of a large density of dangling bonds, typically in the 10^{19}-cm^{-3} range,⁷ hydrogen-free elemental amorphous semiconductors possess a strong subgap absorption. As a consequence, the optical constants and the thicknesses of these films can not be retrieved from optical transmission data with the use of approximate methods, even in cases in which interference fringes are apparent in the spectra. To such a class of thin films we applied the pointwise constrained optimization approach.

We simultaneously deposited a-Ge films (rf-sputtering method) onto Corning 7059 glass and c-Si substrates kept at 200 °C. Two series of samples having thicknesses of ≈ 600 and $\approx 100 \text{ nm}$, respectively, were deposited with a rate of $\approx 1 \text{ Å/s}$. The experimental transmission of the films is shown in Fig. 7. Note that because of the strong optical absorption of crystalline silicon for $\lambda < 1200 \text{ nm}$ and noisy transmission data for $\lambda > 2500 \text{ nm}$, the useful transmission spectral region for the retrieval of the optical constants of a-Ge films deposited onto c-Si is limited to the 1250–2500-nm wavelength range (Fig. 7b).

The way a-Ge films were solved mirrors the previously reported a-Si:H film case. It is unfortunate that we were not successful in all cases. The retrieval process was satisfactory for the $\approx 600\text{-nm}$ -thick film deposited onto c-Si. It failed for films

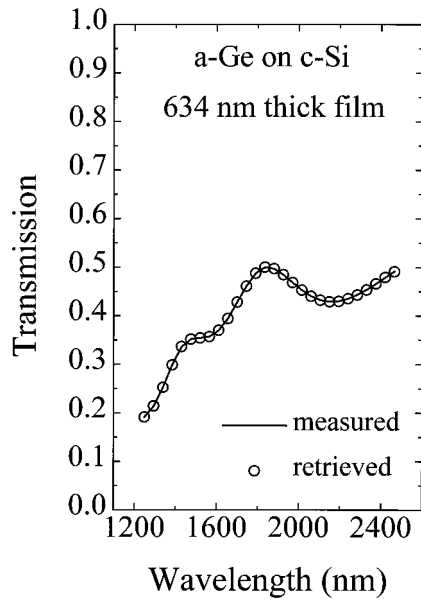


Fig. 8. Optical transmission of the a-Ge/c-Si film No. 2, Fig. 7b, measured in a Perkin Elmer Lambda 9 spectrophotometer (full line) and retrieved transmission (open circles) from the minimization process [expression (13), with $d = 634$ nm].

deposited onto glass substrates, as well as in the case of the very thin (≈ 100 nm) a-Ge film deposited onto c-Si. We discuss these cases separately.

- ≈ 600 -nm-thick a-Ge/c-Si: The optimization process considered transmission data every 5 nm, with a total of 251 nonlinear equations. The experimental transmission spectrum of the film is shown in Fig. 8. In the 1250–2500-nm wavelength range both α and n of a-Ge films are decreasing and convex functions of (λ) (Ref. 20) and constraints (9)–(12) were used. The initial guess considered $3.5 < n < 5.5$, an index range taken from the literature.²¹ The index of refraction of the c-Si substrate was estimated with the help of Eq. (7). The minimization process gave $d = 634$ nm. The values of the retrieved optical constants are shown in Fig. 9. They are compared with those reported by Connell *et al.*²⁰ on rf-sputtered a-Ge films deposited at 350 °C and obtained by a combination of reflectance, transmittance, and ellipsometric measurements. At this point note that, to a certain extent, the optical constants of a-Ge films depend on deposition method, conditions, and substrate temperature. Figure 9 indicates that the values of n and α that are retrieved from optical transmission data compare well only with those of Connell *et al.*²⁰ even though the present films were deposited at a different temperature and under different conditions. Figure 8 shows the goodness of the optical transmission retrieval in the spectral range under consideration. The minimization process, expression (13), for this a-Ge/c-Si film gave an overall error of $\approx 2 \times 10^{-5}$ at $d = 634$ nm.

- ≈ 100 -nm-thick a-Ge/c-Si: The transmission spectra of this film shown in Fig. 7b is nearly flat in the 1250–2500-nm wavelength region. The absence

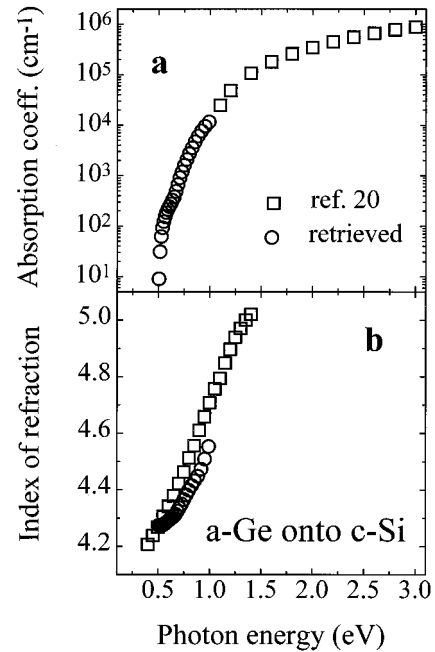


Fig. 9. a, Absorption coefficient, and b, index of refraction of the 634-nm-thick a-Ge film deposited onto c-Si (film No. 2, Fig. 7b); the retrieved optical constants are compared with values from the literature on rf-sputtered a-Ge deposited at 350 °C (Ref. 20).

of any structure in the transmission curve induces in the minimization process, expression (13), the appearance of several local minima of nearly the same value. In other words, a true apparent minimum like that shown in Fig. 5 does not come out of the thickness optimization. The failure is an indication of the limitations of the retrieval process within the context of the adopted constraints on n and α .

- ≈ 600 -nm and ≈ 100 -nm-thick a-Ge/glass: If we look at the transmission spectra of these films (see Fig. 7), we find no apparent reason to explain the failure of the retrieval process. The spectra look well behaved, smooth, and as if they contain enough transmission features in the 600–2000-nm wavelength range. Despite this favorable aspect, all minimization process attempts ended with either a non-well-defined minimum or with retrieved optical constants that do not correspond to a-Ge. We believe that the reason behind the retrieval failure stems from the fact that the a-Ge films deposited onto glass at 200 °C are not homogeneous. In other words, Eq. (1) used in the minimization process does not represent the physical situation that corresponds to the measured optical transmission of a-Ge/glass films. An abundant literature exists that supports this suggestion. Donovan *et al.*,²² Fuhs *et al.*,²³ and the work at Harvard University²¹ on sputtered a-Ge indicate that there is always a void structure in a-Ge films. The size, orientation, and density of such voids depend strongly on deposition temperature and, particularly, on the nature of the substrate. Our own experience on rf-sputtered a-Ge films corroborates these studies.²⁴ It is important to say here that transmission spectra of hydrogenated amorphous germanium (a-Ge:H) films

of various thickness deposited onto glass could not be solved correctly with the present method, most probably because of film inhomogeneity. We conclude that under similar deposition conditions (those used to prepare the films under discussion) the void structure of a-Ge films deposited onto c-Si substrates is much smaller than that of films deposited onto glass substrates. The void structure of a-Ge/c-Si films does not prevent the minimization process from correctly operating on transmission data. The above discussion might also be interpreted as meaning that the pointwise constrained optimization approach discussed here could give relevant information on the homogeneity of thin films.

5. Comparison with Approximate Methods

The simple method proposed by Swanepoel⁵ has been used largely for the problem of estimating the thickness, the absorption coefficient, and the refractive index of thin solid films with transmission data. This method can be applied only to situations in which a relatively large transparent zone exists in the spectrum of relatively thick films so that the transmission curve exhibits some critical points (maximizers or minimizers, see Figs. 1 and 4). The idea is that information measured at these critical points provides sufficient elements to compute good approximations of the thickness and the refractive index at these points. The approach can be justified from both the physical point of view and from purely mathematical arguments based on curve analysis.

Swanepoel⁵ provides a practical procedure for the

estimation of d , $n(\lambda_1^*)$, \dots , $n(\lambda_p^*)$, where $[\lambda_1^*, T(\lambda_1^*)]$, \dots , $[\lambda_p^*, T(\lambda_p^*)]$ are the critical points of the measured function $T(\lambda)$. Then Swanepoel's algorithm proposes to fit the function $n(\lambda) = A\lambda^{-2} + B\lambda + C$ to the data $n(\lambda_1^*)$, \dots , $n(\lambda_p^*)$. The coefficients A , B , and C are estimated with ordinary least squares. In this way the whole function $n(\lambda)$ is estimated and then, for each measured $[\lambda_i, T(\lambda_i)]$, the absorption coefficient $\alpha(\lambda_i)$ may be estimated. It is fortunate that Eq. (8) has only one solution $\alpha(\lambda_i)$ if all the other parameters are given, as is now the case. This solution is easy to obtain for each λ_i and the calculation of $\alpha(\lambda_i)$ is complete for all λ_i . If the film satisfies the condition of having a large transparent region and many critical points, Swanepoel's method is usually accurate in the retrieval of d and $n(\lambda)$ in the transparent region. Therefore if the real $n(\lambda)$ is a quadratic function of $1/\lambda$, the estimation of the optical constants in the whole spectral range should also be accurate.

Problems may arise, however, when $n(\lambda)$ is not exactly quadratic with $1/\lambda$, as may happen with real films. To illustrate the point we consider the two films presented here, which may be analyzed with approximate methods: the 600-nm-thick gedanken film and the 625-nm-thick a-Si:H film. (see Fig. 2, film No. 2, and Fig. 4). First we calculated the transmission for the gedanken film in the 600–2000-nm wavelength range. Then, following the procedure outlined in Ref. 5, we calculated the thickness and the

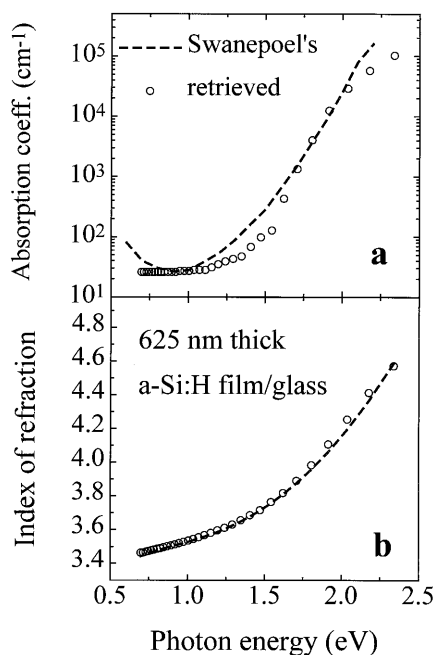


Fig. 10. Optical constants of the a-Si:H film of Fig. 4 (dashed line) as retrieved with the approximate method of Swanepoel⁵ (dashed line). The open circles indicate the retrieval obtained with the present method. Note the accuracy of the retrieval of the index of refraction, b; the approximate methods normally fail in the retrieval of the absorption coefficient, a.

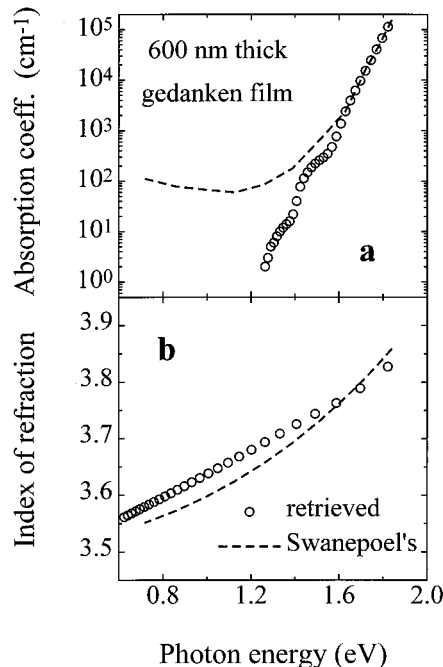


Fig. 11. Optical constants of the gedanken film No. 2, Fig. 2, calculated with Swanepoel's method⁵ (dashed line). For the approximate method to be applicable, optical transmission data were calculated up to a wavelength $\lambda = 2000$ nm. The optical constants estimated with the present method are displayed for comparison (open circles). The retrieval of n and α from Swanepoel's method⁵ is less good than in the case of the a-Si:H film shown in Fig. 10.

index of refraction in the transparent region for both the gedanken and the a-Si:H films. Figures 10 and 11 illustrate the results. The retrieval of the index of the a-Si:H film is good. The best fit to the estimated n values was given by the function

$$n(\lambda) = 4.783 - 3.72 \times 10^{-4}\lambda - 1722/\lambda + 9.135 \times 10^5/\lambda^2,$$

used to extrapolate n to the absorbing region. The thickness retrieved from the approximate method for this well-behaved a-Si:H film is 627.3 nm, in excellent agreement with the minimization pointwise constrained optimization approach. The fit, although reasonable, appears less good for the gedanken film (Fig. 11). The comparison of the absorption coefficient shows that the retrieval with approximate methods is relatively good in the $10^3 > \alpha > 10^5 \text{ cm}^{-1}$ range, but it fails at small α .

It is needless to say that approximate methods are unable to retrieve the thickness and the optical constants of films like the a-Ge (Fig. 8) or the gedanken film No. 1 (Fig. 2).

6. Conclusions

We introduce a new method to estimate the optical constants and the thickness of thin films from optical transmission data only. To solve the problem a pointwise constrained optimization approach is used. The method consists of defining a nonlinear programming problem, the unknowns of which are the coefficients to be estimated, with linear constraints that represent prior knowledge about the physical solution. The method applies to all kinds of transmission spectra and does not rely on the existence of fringe patterns or transparency. The reliability of the new method has been demonstrated with the resolution of gedanken films. It was also applied to homogeneous a-Si:H and to a-Ge films. The estimated optical constants were compared with experimental values that were determined with independent methods on the same films or with data taken from the literature. The agreement was very good in all cases. We believe that the present approach opens new perspectives in thin-film optics, in particular, the characterization of very thin dielectric films currently used in microelectronics.

We are indebted to S. Wagner and S. Theiss, Princeton University, for the deposition and characterization of a-Si:H thin films. We also thank R. Collins and P. Rovira, Pennsylvania State University, for ellipsometric measurements of the a-Si:H/c-Si film. This research has been partially supported by the Brazilian agencies Fundação de Amparo a Pesquisa do Estado de São Paulo (FAPESP), Conselho Nacional de Pesquisas (CNPq), and Programa de Apoio ao Desenvolvimento Científico e Tecnológico (CNPq).

References

1. O. S. Heavens, *Optical Properties of Thin Solid Films* (Dover, New York, 1991).
2. M. Born and E. Wolf, *Principles of Optics*, 6th ed. (Pergamon, London, 1980).
3. A. M. Goodman, "Optical interference method for the approximate determination of refractive index and thickness of a transparent layer," *Appl. Opt.* **17**, 2779–2787 (1978).
4. J. C. Manifacier, J. Gasiot, and J. P. Fillard, "A simple method for the determination of the optical constants n , k and the thickness of a weakly absorbing film," *J. Phys. E* **9**, 1002–1004 (1976).
5. R. Swanepoel, "Determination of the thickness and optical constants of amorphous silicon," *J. Phys. E* **16**, 1214–1222 (1983); see also "Determination of surface roughness and optical constants of inhomogeneous amorphous silicon films," *J. Phys. E* **17**, 896–903 (1984).
6. J. E. Dennis and R. B. Schnabel, *Numerical Methods for Unconstrained Optimization and Nonlinear Equations* (Prentice-Hall, Englewood Cliffs, N.J., 1983).
7. N. F. Mott and E. A. Davis, *Electronic Processes in Non-Crystalline Materials*, 2nd ed. (Oxford U. Press, Oxford, UK, 1979).
8. R. Fletcher, *Practical Methods for Optimization* (Wiley, Chichester, UK, 1987).
9. P. E. Gill, W. Murray, and M. H. Wright, *Practical Optimization* (Academic, London, 1981).
10. R. B. Murtagh and M. A. Saunders, *MINOS User's Guide*, Report SOL 77-9, 1977 (Department of Operations Research, Stanford University, Calif.).
11. R. B. Murtagh and M. A. Saunders, "Large scale linearly constrained optimization," *Math. Programming* **14**, 41–72 (1978).
12. J. Tauc, "Absorption edge and internal electric fields in amorphous semiconductors," *Mater. Res. Bull.* **5**, 721–730 (1970).
13. G. A. N. Connell, "Optical properties of amorphous semiconductors," in *Amorphous Semiconductors*, M. H. Brodsky, ed., Vol. 36 of Topics in Applied Physics (Springer-Verlag, Berlin, 1979), pp. 73–111.
14. R. A. Street, *Hydrogenated Amorphous Silicon* (Cambridge U. Press, Cambridge, UK, 1991).
15. G. D. Cody, "The optical absorption edge of a-Si:H," in *Hydrogenated Amorphous Silicon*, J. Pankove, ed., Vol. 21B of Semiconductors and Semimetals Series, R. K. Willardson and A. C. Beer, eds. (Academic, New York, 1984), pp. 11–82.
16. W. B. Jackson, N. M. Amer, A. C. Boccarda, and D. Fournier, "Photothermal deflection spectroscopy and detection," *Appl. Opt.* **20**, 1333–1344 (1981).
17. S. H. Wemple and W. DiDomenico, "Behavior of the electronic dielectric constant in covalent and ionic materials," *Phys. Rev. B* **3**, 1338–1351 (1971).
18. S. H. Wemple, "Refractive-index behavior of amorphous semiconductors and glasses," *Phys. Rev. B* **7**, 3767–3777 (1973).
19. D. T. Pierce and W. E. Spicer, "Electronic structure of amorphous silicon from photoemission and optical studies," *Phys. Rev. B* **5**, 3017–3029 (1972).
20. G. A. N. Connell, R. J. Temkin, and W. Paul, "Amorphous germanium, III. Optical properties," *Adv. Phys.* **22**, 643–665 (1973).
21. W. Paul, G. A. N. Connell, and R. J. Temkin, "Amorphous germanium, I. A model for the structural and optical properties," *Adv. Phys.* **22**, 531–580 (1973).
22. T. M. Donovan and K. Heinemann, "High resolution electron microscope observation of voids in amorphous Ge," *Phys. Rev. Lett.* **27**, 1794–1796 (1971).
23. W. Fuhs, H.-J. Hesse, and K. H. Langer, "Substrate specific voids in amorphous germanium," in *Amorphous and Liquid Semiconductors*, J. Stuke and W. Brenig eds. (Taylor and Francis, London, 1974), pp. 79–84.
24. M. Mulato, I. Chambouleyron and I. Torriani, "Hydrogen bonding and void microstructure of a-Ge:H films," *J. Appl. Phys.* **76**, 4453–4455 (1996).